

GUGGENHEIM AERONAUTICAL LABORATORY

CALIFORNIA INSTITUTE OF TECHNOLOGY

DESIGN AND PERFORMANCE OF A SIMPLE
INTERFEROMETER FOR WIND TUNNEL MEASUREMENTS

Harry L. Ashkenas & Arthur E. Bryson

PASADENA, CALIFORNIA

DESIGN AND PERFORMANCE OF A SIMPLE
INTERFEROMETER FOR WIND TUNNEL MEASUREMENTS

Harry I. Ashkenas* and Arthur E. Bryson**

ABSTRACT

The design of an interferometer with a 3 1/2" diameter light field and its application to a continuously operating 4" x 10" supersonic wind tunnel are discussed. The main features of this interferometer are (1) its very low cost compared to previous designs, (2) its light weight and flexibility, (3) a simple device permitting the instrument to be used also as a Schlieren system, and (4) its unique feature of passing both light beams through the test section to minimize the effect of the side wall boundary layers in the interferograms.

INTRODUCTION

During the past few years the Mach-Zehnder interferometer has come into increased use throughout this country for investigating high speed aerodynamic phenomena. Ladenburg and his co-workers at Princeton University have been particularly active in this field (see Refs. 1 to 7). The main attraction of the instrument for the

*Graduate Assistant, California Institute of Technology, now at Cornell University.

**Graduate Assistant, California Institute of Technology.

aerodynamicist is its ability to provide quantitative data on the density distribution for the complete flow field under investigation without the necessity of inserting probes into the flow (which introduce changes in the flow and require many measurements to describe the complete flow field). The bibliography at the end of this paper lists references giving ample information on the optical theory of the instrument and describing its application to the study of two-dimensional and axially symmetric flow fields.

In the course of work on boundary layer - shock wave interaction at GALCIT,* it became apparent that an interferometer could be used to great advantage. However the location and physical set-up of the GALCIT 4" x 10" Transonic Wind Tunnel are highly unfavorable for the use of an interferometer according to standard concepts: the tunnel is continuously operating, the test section being directly above two 300 hp. centrifugal blowers; the power plant of the GALCIT 10 ft. Wind Tunnel is quite close to the test section room; the floor of the test section room is of temporary wood construction. Thus the vibration and noise levels near the test section are unusually high. The main problem, therefore, in the design of the interferometer was to obtain proper vibration isolation. Furthermore it was required that the interferometer be mounted and removed easily to make room for other set-ups (such as Schlieren) and also to make possible easy changes to the test section. (For details of the wind tunnel see

*Guggenheim Aeronautical Laboratory, California Institute of Technology.

Refs. 43 and 44.) The tunnel has a flexible nozzle and variable second throat permitting operation from $M = 0.7$ to $M = 1.5$.

The instrument developed is comparatively very simple and has proved to be quite adequate. It is believed that a description of the design and installation of the interferometer will be useful since similar problems will probably arise with other wind tunnels.

The instrument was designed and built during the course of an investigation which was begun under Air Force sponsorship but which, for the past year, has been carried out under the sponsorship of the National Advisory Committee for Aeronautics.

The authors wish to thank Dr. Hans Wolfgang Liepmann who started them on the design and whose idea it was to put both light beams through the test section. They also wish to thank Mr. Satish Dhawan who suggested and designed the Schlieren attachment to the instrument.

DIFFERENCES FROM PERVIOUS INTERFEROMETERS

The principal innovations of this interferometer are believed to be (1) its low cost, (2) its light weight and simplicity of construction, (3) its simple attachment for taking Schlieren pictures, and (4) its feature of passing both light beams through the test section.

The appendix contains an itemized cost estimate for the interferometer; it should be noted that the cost of reproducing the instrument now would be considerably less, mainly due to the elimination of the engineering time.

A rather thick boundary layer exists on the test section windows

so that if only one beam traversed the test section a large error would be introduced due to the fact that the interferometer integrates the value of density through the flow. Most of the previous interferometers put one beam through the flow being investigated and the other beam through a glass-paneled compensating chamber in which the air density can be adjusted to approximately the free stream density of the flow. In this interferometer, both beams traverse the test section, one passing through the flow being investigated, the other passing through the test section $7 \frac{3}{4}$ " ahead of that beam; the boundary layer does not change its thickness appreciably in the distance between the two beams, so that both beams traverse effectively the same boundary layers and the latter's effects are thus cancelled. At the same time the flow in the front beam corresponds to an "automatic compensating chamber" providing free stream density as the basis for the fringe shifts. This is particularly applicable to supersonic flow where the flow ahead of the disturbance is uniform, but it can also be used for subsonic flows where the effect felt ahead of the model is small.

OVER-ALL DESCRIPTION OF THE INTERFEROMETER

1. Optical Path

A schematic diagram of the optical path through the instrument is shown in Fig. 1. Light from a mercury vapor lamp is passed through a filter and focused by a lens on a small mirror which is at 45° to the incident beam; this small mirror is also at the focus of a parabolic mirror causing the reflected light to be parallel.

This parallel beam is passed back over the small mirror (which shows up as a slight shadow on the interferograms but does not interfere at all in their evaluations) and is then split at the half silvered mirror #1 into two beams; one beam passes through mirror #1, reflects off the fully silvered mirror #3, then passes through the test section ahead of the model; the other beam reflects from mirror #1, passes through the test section over the model, then reflects from the fully silvered mirror #2. The two beams are recombined at the half-silvered mirror #4 and are brought to a focus by a spherical mirror on a ground glass screen. The plane mirrors are at the corners of a $7 \frac{3}{4}$ " x $35 \frac{3}{4}$ " rectangle, the plane of the rectangle being horizontal. The light beams are circular and can be varied in diameter from 2" to $3 \frac{1}{2}$ " by varying the position of the lens; both beams pass through the 12" diameter test section windows which are made of good quality plate glass of 1" thickness. (The use of plate glass instead of high quality plane-parallel optical glass provides a substantial reduction in cost; it was found that there was no need for the latter.) The instrument can be traversed forward and backward as well as up and down so that the small field of view is not a disadvantage; actually, most of the phenomena studied are local flow phenomena which are adequately covered by the $3 \frac{1}{2}$ " diameter light field. Other test section window arrangements for studying various types of flows are being designed.

2. Light Source

The interferometer has been designed with a minimum of air-glass interfaces to prevent loss of light, there being only four

such surfaces, two at the lens, and two at the filter; these surfaces are coated to prevent further loss of light. As a result of this design a 100 watt mercury light can be used and in conjunction with the filter it gives sufficient monochromatic light for pictures to be taken at $1/800^{\text{th}}$ of a second. (Figs. 5-8 were taken with this light source at exposures of $1/400^{\text{th}}$ or $1/800^{\text{th}}$ of a second.)

3. Mounting

The four plane mirrors, the light source, the paraboloidal mirror, and the spherical mirror are mounted on a wooden box which is suspended from a welded pipe framework by four sets of eight rubber bands each. The box with all the equipment mounted on it weighs only 250 lbs. which is in contrast to all other interferometers that have come to the authors' attention where the mirror base plates have been very massive to provide rigidity; here the box is allowed to deflect in any manner it chooses and once it has assumed its deflected position and the mirrors have been adjusted, the shock mounting of the system effectively prevents any further misalignment from taking place. The action of the rubber bands rubbing over each other provides sufficient damping for the system. The natural frequency of the box is about 1 cycle per second; this was found to provide not quite enough vibration isolation and so the frame has also been isolated by placing 12" of foam rubber under each of the four corners and this has provided sufficient vibration isolation to permit one to see the fringes while running the wind tunnel (two 300 hp. centrifugal compressors power the tunnel) and also while the GALCIT 10 ft. Wind Tunnel is running (its 750 hp. motor and fan are quite

near the interferometer). The rubber bands are attached to jack screws permitting the box to be traversed in a vertical direction and allowing a fine vertical adjustment to be made in getting the light beam parallel to the surfaces of two-dimensional models. The whole interferometer can be traversed along the test section on four casters; it can also be rotated through small angles on these casters allowing a fine horizontal adjustment to be made in getting the light beam parallel to the surfaces of two-dimensional models. The interferometer can also be completely traversed away from the test section and the regular Schlieren system traversed into its place. (Although Schlieren pictures can be taken with the interferometer as described below, these pictures are not of such high quality as those taken with the regular Schlieren system.)

The camera box is mounted on the pipe frame so that putting film holders in the camera does not disturb the instrument's adjustment.

4. Adjustments

The various component parts of the interferometer are fitted with a large number of adjustments. This practice, while giving rise to a large number of possible misalignments, also results in considerable ease in setting up the instrument. Locking devices are present to prevent any change in the final set-up.

DETAILED DESCRIPTION OF COMPONENT PARTS

1. Monochromatic Light Source

The monochromatic light source is a mercury vapor lamp, General Electric Type AH-4, housed in a Cenco #87269 lamp housing. The lamp

house is attached to a brass tube which contains a Bausch and Lomb achromatic coated lens of 142.9 mm focal length and 46.0 mm diameter. The brass tube also contains a receptacle for a Wratten No. 77A filter which filters out the green line at $5461 \overset{\circ}{\text{Å}}$ in the mercury spectrum. Attached to the top of the brass tube is a U-frame which supports a rectangular frame on which a small diameter wire is mounted carrying the 2 x 4 mm first surface plane mirror which acts as a secondary light source since it is at the focus of a 5 1/2" diameter, 15" focal length paraboloidal mirror. The paraboloidal mirror is mounted in an aluminum mirror cell of the type described by Strong in Ref. 21; a central flexure post and four adjusting screws provide the fine adjustment of position, while the course adjustment of position is provided by the sliding tubular mounting that is attached to the interferometer box.

2. White Light Source

A 2" x 2" first surface plane mirror has been mounted on a hinge in the mercury lamp housing and a hole cut out of the housing so that by turning a screw the mirror is brought to a position that is at 45° to the light from a 500 watt motion picture projector lamp that is mounted adjacent to the lamp housing; this light source is the same distance from the mirror as the mercury light so that both sources are optically at the same point with respect to the lens (see Fig. 1).

3. Plane Parallel Mirrors

The plane parallel mirrors are carried in a frame which is shown in Fig. 4. Each mirror itself is held in a split brass ring by means of a soft rubber, full circumference support. Two gimbals allow

rotation of the mirror about a horizontal and vertical axis. Rotation of the gimbals is obtained by means of remotely controlled, reversible electric clock motors. The output shaft of these motors (Haydon #3200) makes one revolution per eight days resulting in an extremely fine control of the angular displacements of the mirrors. The gear box on the motor is equipped with stamped metal gears, and a not inconsiderable amount of backlash is present, hence a simple torsion spring is placed at each bearing to supply a backlash-eliminating force.

The frames of all four mirrors are identical. Duralumin castings are used for the outer frame and the inner gimbals. There is no provision for coarse angular adjustment of the mirrors which makes the initial adjustment somewhat tedious but thereafter no coarse adjustment is needed. Mirrors #1, #2, and #3 (see Figs. 2 and 3) are bolted to the top of the plywood box. Mirror #4 is mounted on a traversing table to provide the adjustment for equalizing the optical path lengths of the two arms of the interferometer. The traversing mechanism features a Le Blond, lathe bed type way, a traversing screw of 1 mm pitch, driven by a hand operated 50:1 worm gear reduction unit, a simple nut, and a pin-driven gravity-emplaced traversing table.

4. Camera and Schlieren System

The photographic components consist of a 3 1/2" diameter, 24" focal length spherical mirror, and Eastman Synchro-Rapid 800 shutter (speeds up to 1/800th of a second), and a 4" x 5" Graphic camera back with a ground glass viewing screen. Due to the shutter's small

diameter it has been placed at the end of a truncated conical piece extending from the camera box (see Fig. 3). The focal point of the light beam reflected from the spherical mirror is just inside the shutter in the conical part of the camera and a micrometer with a razor blade mounted on its end is placed there as the knife edge of a Schlieren system; the knife edge can be traversed along the light beam to obtain best sensitivity and it can be rotated to give "knife edge horizontal" and "knife edge vertical" pictures. To take Schlieren pictures the forward light beam of the interferometer is blocked out, the filter removed, and the white light source is used.

The film used is Ansco Triple-S-Pan which is sufficiently fast to take good pictures at $1/400^{\text{th}}$ of a second. Slightly better pictures are obtained using Eastman 103-G spectroscopic plates which are especially sensitive in the green range containing the wavelength of the monochromatic light used ($5461 \overset{\circ}{\text{A}}$): these plates are fast enough for pictures at $1/800^{\text{th}}$ of a second and have the added advantage that there is no film shrinkage which could cause errors in fringe shift measurement. (Actually, by comparing the film and the glass plates no significant errors in fringe shift measurement have been found.)

PERFORMANCE OF THE INTERFEROMETER

1. Initial Adjustment

The initial adjustment of the interferometer was made using the pentaprism method as described in Ref. 30. This adjustment required

several days to perform due to the slow mirror movements, but once completed it does not have to be done again.

2. Daily Adjustment

Due to slight deflections of the box caused by temperature and humidity changes, the interferometer gets slightly out of adjustment from day to day. However, with an experienced operator, fringes of the desired spacing and orientation can be focused on the ground glass screen in less than ten minutes using the "near and far cross-hair" method of adjustment described in Ref. 30; for this an auxiliary plane mirror is placed at 45° to the light beam just ahead of the spherical mirror and an auto-collimating telescope is placed in the reflected beam from this mirror; if the telescope has been previously focused on a very distant object, it will now focus on the two images of the secondary light source (the 2 x 4 mm mirror) if the light is parallel. These images serve as the "far cross-hairs" being optically at infinity; the "near cross-hairs" are the shadows of this 2 x 4 mm mirror, which is only a few inches from the half-silvered mirror #1. Now, focusing on the "far cross-hairs", mirror #1 is rotated about its vertical and horizontal axes until the two images coincide; then, focusing on the "near cross-hairs", mirror #4 is rotated about its horizontal and vertical axes until these two images coincide. This latter adjustment slightly disturbs the previous adjustment of mirror #1 which is then done over again, and similarly then mirror #4 is readjusted; this process is rapidly convergent, usually requiring only the first adjustment of each mirror.

3. Horizontal or Vertical Fringes

The geometry of this particular interferometer is such that by

now rotating both mirror #1 and mirror #4 in the same direction about horizontal (or vertical) axes in a ratio of 7 to 5, horizontal (or vertical) fringes appear very nearly in the plane of the ground glass screen. The spherical mirror is rotated slightly, placing the reflected beam outside the camera so that a white card can be placed in the beam to determine the plane in which the fringes are focused. By reference to the "linear interferometer representation" described in Ref. 34, the operator can then tell which way to rotate mirrors #1 and #4 to focus the fringes precisely on the ground glass screen with the desired spacing and orientation. Previously the spherical mirror has been located so as to focus a plane that is $1/3$ of the way from the exit window to the entrance window on the ground glass screen; this minimizes refraction errors in the interferogram (see Ref. 7). Thus both model and fringes are in focus on the ground glass screen.

4. Equalizing Optical Path Lengths

The next adjustment is to equalize the optical path lengths in the two legs of the interferometer; this is done by placing an auxiliary mirror in front of the paraboloidal mirror so that it cuts out half of the monochromatic light beam; an auxiliary white light source is then reflected onto this auxiliary mirror so that its light travels the same circuit as the monochromatic light. The image formed near the ground glass screen is then half monochromatic light fringes and half white light field. Mirror #4 is then traversed until the white light fringes appear in the white light field; usually only a few turns of the traversing wheel are required and

often the white light fringes have not "strayed" since the last use of the interferometer; the correct direction to traverse is easily checked by the fact that the monochromatic fringes should get more "contrasty" if the traversing is done in the correct direction.

5. Eliminating "Twist"

The next adjustment is to eliminate "twist" from the beam, i.e. to place the two images directly above each other (for the case of horizontal fringes); this gives the maximum contrast in the fringes. This can be done by rotating mirrors #1 and #4 about their vertical axes slightly (for the case of horizontal fringes) until the monochromatic fringes are parallel to the white light fringes and they are both horizontal; this adjustment works only if divergent white light is used in the auxiliary beam. Getting rid of "twist" can also be done by trial and error without the white light by simply rotating about the vertical axes (as above) until the fringes appear to have maximum contrast.

6. Infinite Fringe Adjustment

The infinite fringe adjustment is obtained by first making the adjustment above for either vertical or horizontal fringes and then slowly increasing the fringe spacing keeping the fringes focused on the ground glass screen (this is easily done by rotating mirrors #1 and #4 in the same direction in a ratio of 7 to 5).

7. Aligning Light Beam to Models

The final adjustment is to align the light beam to the surface of two-dimensional models or, in the case of axially symmetric models, to align the light beam perpendicular to the axis of symmetry.

8. Procedure During a Run

Before the tunnel is turned on, an undisturbed fringe picture is taken. Then after the flow has been turned on and has reached an equilibrium flow condition, the monochromatic fringe pictures are taken; while still running, the filter is removed, the mirror in the lamp housing is rotated into place and the white light then becomes the light source; the white light fringe picture is then taken. Next the front beam of the interferometer is blocked out and the Schlieren system adjusted, then a Schlieren picture is taken. A shadowgram can also be taken at this point if desired, simply by moving the knife edge back out of the beam. All of these operations can be performed in a very few minutes so that a minimum of tunnel time is used for each run.

9. Evaluation of Interferograms

Knowing the stagnation temperature and pressure in the settling chamber and the Mach number in the test section the density of the air in the front beam is readily calculated by the isentropic flow relations. If in addition we know the span of the model, the wave length of the light used, and the Gladstone-Dale constant for this wave length, the interferogram can then be completely evaluated to give the density distribution throughout the entire flow field about the model.

For two-dimensional flows, the evaluation is particularly simple since the density change is directly proportional to the distance the fringes shift from their undisturbed positions. By comparing the fringe pictures taken with and without flow this fringe shift can be

determined. A particularly simple way of doing this, mentioned in Ref. 18, is to superimpose the negatives of these two pictures; faint lines then appear which are lines of constant fringe shift. Since the negatives are small this can not be done too accurately if the fringe spacing is quite narrow; to get over this difficulty enlarged transparencies of the undisturbed fringe pictures are made; placing this transparency on the enlarger table, the other picture is focused until the two pictures "line up", i.e. the fringes ahead of the shock wave fall on top of each other. Then the printing paper is put under the transparency and a picture is printed giving the lines of constant fringe shift as shown in Fig. 7. To determine the proper number of fringe shifts associated with each line, the white light picture must be used to trace the central fringe through the shock wave or the fringe shift at a pressure tap on the model is calculated.

The infinite fringe picture serves as a check on the above method, but its accuracy is dependent on the accuracy with which the mirrors were made so that it is usually only accurate (for this interferometer) within $\pm 1/2$ fringe shifts. The method of finite fringes above "calibrates out" the inaccuracies of the optical system.

The evaluation for axially symmetric flows is described in Ref. 1; it is considerably more difficult and tedious than the evaluation for two-dimensional flows since the fringe shift is related to the density change by an Abel integral equation.

10. Obtaining Two-Dimensional Flows

One difficulty in the use of the interferometer for two-dimensional flows is that two-dimensional flows are very difficult, if

not impossible, to obtain, and consequently errors are introduced into the interferogram. As previously described, passing both beams through the test section is a help in overcoming this difficulty by minimizing boundary layer effects. Permitting models to span the tunnel only up to the beginning of the side wall boundary layers seems to minimize the three-dimensional effects although this has not been thoroughly checked as yet. The three-dimensional, or "tip" effects, probably vary considerably with the model being used and with the flow velocity; also the interaction of the shock waves with the side wall boundary layers alters the tip effects and the boundary layers. The tip effects and the shock wave - boundary layer interaction effects can not be separated and must be considered together in determining the accuracy of the interferograms. Preliminary tests on detached shock waves indicate that both boundary layer and three-dimensional effects are practically eliminated by careful choice of the model span.

CONCLUSION

Figs. 5-10 are typical interferograms taken with this instrument. Fig. 5 is an interferogram showing horizontal undisturbed fringes taken through the test section windows with the wind tunnel turned off. Fig. 6 shows the flow field about a 10° semi-angle wedge with a detached shock wave (the pegs on the flat portion following the wedge are for aid in alignment of the light beam to the leading edge of the wedge). An investigation of the flow field behind such detached shock waves is at present being carried on using

the interferometer. Fig. 7 is an interferogram made by superimposing the negatives of an interferogram with flow and one without flow; the shadowy lines are the lines of $n + 1/2$ fringe shifts (n an integer) and are lines of constant density. Fig. 8 is an interferogram taken with the "infinite fringe" and the dark lines are approximately lines of $n + 1/2$ fringe shifts (n an integer) and are lines of constant density. Fig. 9 is an interferogram taken with white light instead of monochromatic light and shows the manner in which the fringes can be traced through a shock wave. Fig. 10 is a Schlieren picture taken with the special attachment to the interferometer described above.

The performance of this interferometer on the GALCIT Transonic Wind Tunnel has proved quite satisfactory to date and it is hoped that many interesting aerodynamic phenomena may be studied with it in the future.

APPENDIX

COST OF THE GALCIT INTERFEROMETER

Plane-Parallel Plates	\$2000.00
Mirror Frames	75.00
Turning Motors	50.00
Light Source	50.00
Filter	30.00
Lens	18.00
Spherical Mirror	27.50
Paraboloidal Mirror	100.00
Shutter	40.00
Camera Back	18.00
Suspension Frame	34.00
Optical Bench	25.00
Two Test Section Windows	13.00
Traversing Table, Switch Box, Mirror Cells, Rails, Suspension Clamps, etc. -- Shop Labor	1500.00
Temporary Set-Up	40.00
Engineering Time	2000.00
	<hr/>
TOTAL	\$6020.50

BIBLIOGRAPHY

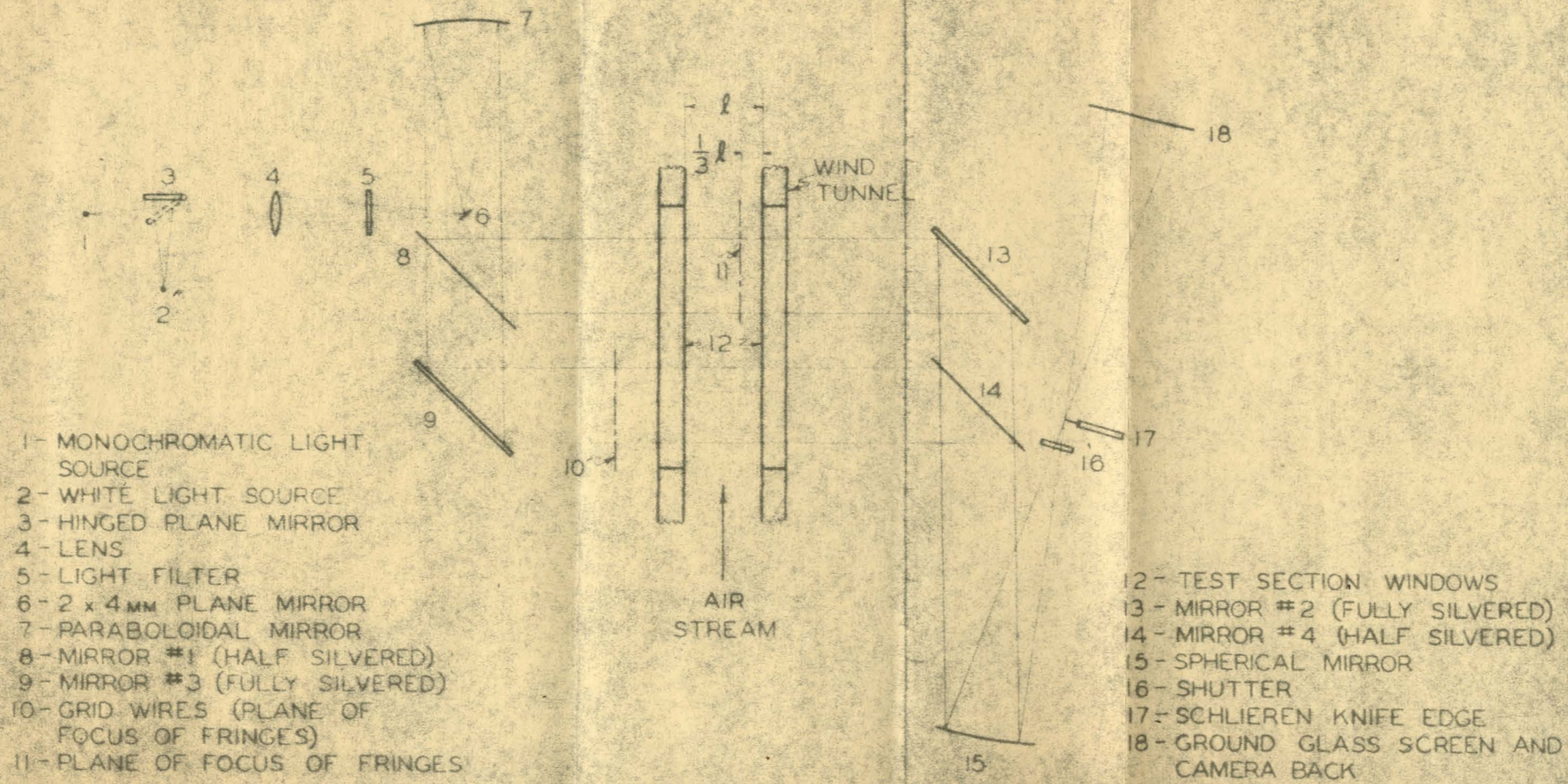
1. Ladenburg, R., Van Voorhis, C. C. and Winckler, J.: Interferometric Study of Supersonic Phenomena Part I, A Supersonic Air Jet at 60 lb./in.² Tank Pressure. Navord Report 69-46, April 17, 1946. Part II, The Gas Flow Around Various Objects in a Free, Homogeneous Supersonic Air Stream. Navord Report 93-46, Sept. 2, 1946. Part III, Boundary Layer and Shock Wave Interactions Observed Along Probes and Wires in Supersonic Air Streams. Navord Report 7-47, Feb. 19, 1947.
2. Ladenburg, Panofsky, Van Voorhis, Winckler: Study of Shock Waves by Interferometry. NDRC Report No. A-332, OSRD No. 5204.
3. Ladenburg, R.: Interferometric Analysis of Supersonic Jets. Navord Report 74-46.
4. Winckler, J.: The Mach Interferometer Applied to Studying an Axially Symmetric Supersonic Air Jet. Review of Scientific Instruments, Vol. 19, No. 5, May 1948.
5. Ladenburg, Winckler, J. and Van Voorhis, C. C.: Interferometric Studies of Faster than Sound Phenomena. Part I, The Gas Flow Around Various Objects in a Free, Homogeneous Supersonic Air Stream. The Physical Review, Vol. 73, No. 11, June 1948. Part II, Analysis of Supersonic Air Jets. The Physical Review, Vol. 76, No. 5, Sept. 1, 1949.
6. Bershader, D.: An Interferometric Study of Supersonic Channel Flow. Review of Scientific Instruments, Vol. 20, No. 4, April 1949.
7. Ladenburg, R. and Wachtell, C. P.: Further Interferometric Studies of Boundary Layers Along a Flat Plate. Palmer Physical Laboratory, Princeton University, Dec. 15, 1949.
8. Zobel, Th.: Fortschritte in Optischer Strömungsmessung. Forschungsbericht, 1934.
9. Zobel, Th.: Verwendung von Lichtinterferenzen in der Technischen Messung. Zeitschrift für Vereines Deutschen Ingenieru, Vol. 81, p. 619, 1937.
10. Zobel, Th.: Development and Construction of an Interferometer for Optical Measurements of Density Fields. NACA T.N. No. 1184.
11. Zobel, Th.: Strömungsmessung durch Lichtinterferenz. Forschungsbericht 1167. Translation NACA T.M. No. 1253, Aug. 1949. (also Wright Field Air Document Div. T-2 and ATI 26165.)

12. Hutton, S. P.: The Use of Interferometers in Aerodynamics. Technical Note No. Aero. 1808 (Restricted), Royal Aircraft Establishment.
13. Groth, E.: Evaluation of Density Fields Around Airfoils in Wind Tunnels by Means of Optical Interference. N.A.A. Report N.A. 8776, Nov. 21, 1945.
14. Groth, E.: Measurement of Flow Around the Airfoil by Means of a Mach-Zehnder Interferometer. Jan. 9, 1946. Joint Intelligence Objectives Agency, Washington, D. C., Aug. 21, 1946, BIGS-94 ADG 1011. Also R & T No. 127, Jan. 1946.
15. Groth, E.: Evaluation of Interferometer Measurements of an Airfoil in the 250 x 250 mm High Speed Tunnel A7. J 10 A - BIGS-98 AGD 1027, Feb. 1946. Also R & T No. 128, Feb. 1946.
16. Groth, E.: Evaluation of Density Fields at High Subsonic Velocities by Means of Optical Interference Measurements. N.A.A. Report N.A. 8783, Nov. 26, 1945.
17. Groth, E.: Sensitivity and Accuracy of the Interference Method Applied to Pressure Measurements in Wind Tunnels. ATI - 36783, AGD 1042.
18. Edelman, G. M.: The Design, Development and Testing of Two-Dimensional Sharp Cornered Nozzles. Meteor Report No. MIT 30
19. Gooderum, P. B., Wood, G. P. and Brevoort, M. J.: Investigation with an Interferometer of the Turbulent Mixing of a Free Supersonic Jet. NACA T.N. No. 1857, April 1949.
20. Heberle, J. W., Wood, G. P. and Gooderum, P. B.: Data on Shape and Location of Detached Shock Waves on Cones and Spheres. NACA T.N. 2000, Jan. 1950.
21. Strong, J.: Procedures in Experimental Physics. Prentice-Hall, 1938.
22. Zehnder: Ein Neuer Interferenzrefraktor. Zeitschrift für Instrumentenkunde, Vol. 11, pp. 275-285, 1891.
23. Mach, L.: Über ein Interferenzrefraktometer. Wiener Berichet, Vol. 101, pp. 5-10, 1892, Vol. 102, pp. 1035-1056, 1893.
24. Mach, L.: Über Einige Verbesserung an Interferenzapparaten. Wiener Berichte, Vol. 107, pp. 851-859, 1898.
25. Hansen, G.: Über ein Interferometer Nach Zehnder-Mach. Zeitschr. f. Tech. Physik, Vol. 12, Nr. 9, pp. 436-440, 1931.

26. Kennard, R. B.: An Optical Method for Measuring Temperature Distribution and Convective Heat Transfer. Bureau of Standards Journal of Research, Vol. 8, pp. 787-805, 1932.
27. Schardin, H.: Theorie und Anwendung des Mach-Zehnderschen Interferenz-Refraktometers. Zeitschrift für Instrumentenkunde Vol. 53, p. 396 and p. 424, 1933. R.A.E. Translation No. 79.
28. Hansen, G.: Über die Ausrichtung der Spiegel bei einem Interferometer nach Zehnder-Mach. Zeitschrift für Instrumentenkunde, Vol. 60, p. 325, 1940.
29. Lamla, E.: Concerning the Light Path in a Mach-Zehnder Interferometer. Jahrbuch 1941 der Deutschen Luftfahrtforschung, pp. 727-736. R.A.E. Translation No. 80.
30. Lamla, E.: Über die Justierung des Mach-Zehnderschen Interferometer. Forschungsbericht Nr. 1924, LFA, Braunschweig, Dec. 31, 1943.
31. Hottenroth: Über Einige Erfahrungen am Mach-Zehnderschen Interferometer. Forschungsbericht Nr. 1924, LFA, Braunschweig, Dec. 31, 1943. (Translated Air Doc. Div. T-2, Ames, Wright Field, RC-1031, F-26635 (ATI 26635).)
32. Clippinger, R. F.: Comparison Between the Jamin-Mach Interferometer and the Williams Interferometer as Applied to the Study of Airflow Around a Supersonic Projectile of Revolution. Ballistic Research Laboratory, Aberdeen Proving Ground, Report No. 567, Sept. 21, 1945.
33. Weyl, F. J.: Analytical Methods in Optical Examination of Supersonic Flow. Navord Report 211-45, Dec. 11, 1945.
34. Kinder, W.: Theorie des Mach-Zehnder Interferometers und Beschreibung eines Gerätes mit Einspiegeleinstellung. Optik, Vol. 1, p. 413, 1946.
35. Winckler, E. H.: Analytical Studies of the Mach-Zehnder Interferometer. N.O.L. Report No. 1077, Dec. 1947.
36. Eckert, E. R. G., Drake, R. M. Jr. and Soehngen, E.: Manufacture of a Zehnder-Mach Interferometer. USAAF T.R. No. 5721, August 1948.
37. Olsen, H. L.: An Interferometric Method of Gas Analysis. University of Wisconsin, CM-514 NORD 9938, Task Wis-1-I, Nove. 1948.
38. Eckert, E. R. G. and Soehngen, E. E.: Studies on Heat Transfer in Laminar Free Convection with the Zehnder-Mach Interferometer. USAAF T.R. 5747, Dec. 1948.

39. Winckler, Jordan: A Mechanical Evaluation Method for Interferometer Photographs. ATI No. 1964.
40. Bleakney, W., Weimer, D. K. and Fletcher, C. H.: Shock Tube; A Facility for Investigation in Fluid Mechanics Research. Review of Scientific Instruments, Vol. 20, No. 11, pp. 807-816, Nov. 1949.
41. Johnson, E. R. and Scholes, J. F. M.: A New Interferometer. Australian Jour. Sci. Research, A, 1, pp. 464-471, Dec. 1948. (#5367 Phys. Abstracts, Vol. 52 #622, Oct. 1949)
42. Ashkenas, Harry I.: The Design and Construction of a Mach-Zehnder Interferometer for Use with the GALCIT Transonic Wind Tunnel. Thesis 1949, California Institute of Technology.
43. Liepmann, H. W.: The 2" x 20" Transonic Wind Tunnel. Final Report for Supplement Agreement No. 1 (S-4843) to Contract No. W 33-038 ac-1717 (11592) with ATSC, Wright Field, 1945.
44. Liepmann, H. W.: The Interaction Between Boundary Layer and Shock Waves in Transonic Flow. Journal of the Aeronautical Sci., Vol. 13, No. 12, Dec. 1946.

FIG. 1 - SCHEMATIC DIAGRAM OF OPTICAL PATH



- 1 - MONOCHROMATIC LIGHT SOURCE
- 2 - WHITE LIGHT SOURCE
- 3 - HINGED PLANE MIRROR
- 4 - LENS
- 5 - LIGHT FILTER
- 6 - 2 x 4 MM PLANE MIRROR
- 7 - PARABOLOIDAL MIRROR
- 8 - MIRROR #1 (HALF SILVERED)
- 9 - MIRROR #3 (FULLY SILVERED)
- 10 - GRID WIRES (PLANE OF FOCUS OF FRINGES)
- 11 - PLANE OF FOCUS OF FRINGES

- 12 - TEST SECTION WINDOWS
- 13 - MIRROR #2 (FULLY SILVERED)
- 14 - MIRROR #4 (HALF SILVERED)
- 15 - SPHERICAL MIRROR
- 16 - SHUTTER
- 17 - SCHLIEREN KNIFE EDGE
- 18 - GROUND GLASS SCREEN AND CAMERA BACK

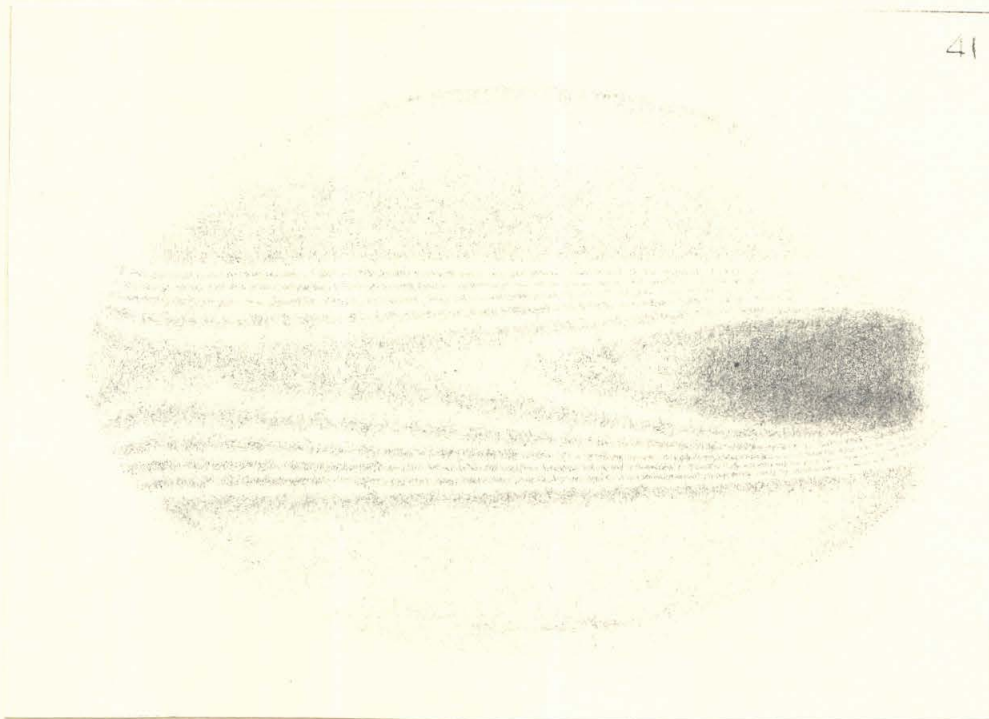


Fig. 2 - North Half of the Interferometer Mounted on the GALCIT Transonic Wind Tunnel Showing Parabolic Mirror, Plane Parallel Mirrors #1 and #3, and the Vibration Mounting.

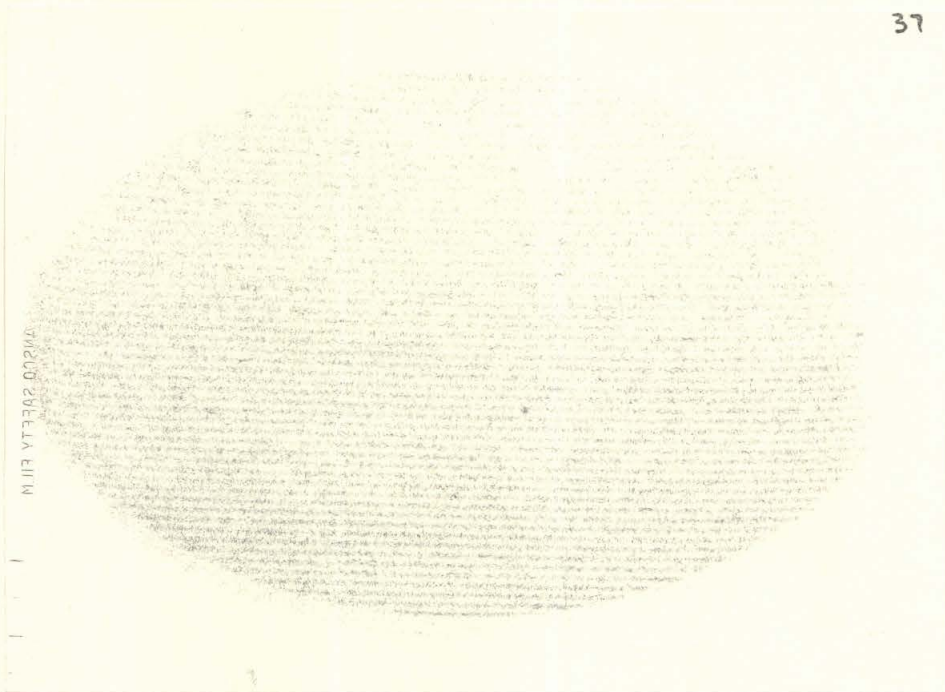


Fig. 3 - South Half of the Interferometer Showing the Plane-Parallel Mirrors #2 and #4, the Spherical Mirror, the Shutter, the Micrometer Knife-Edge for Schlieren Pictures, and the Camera.

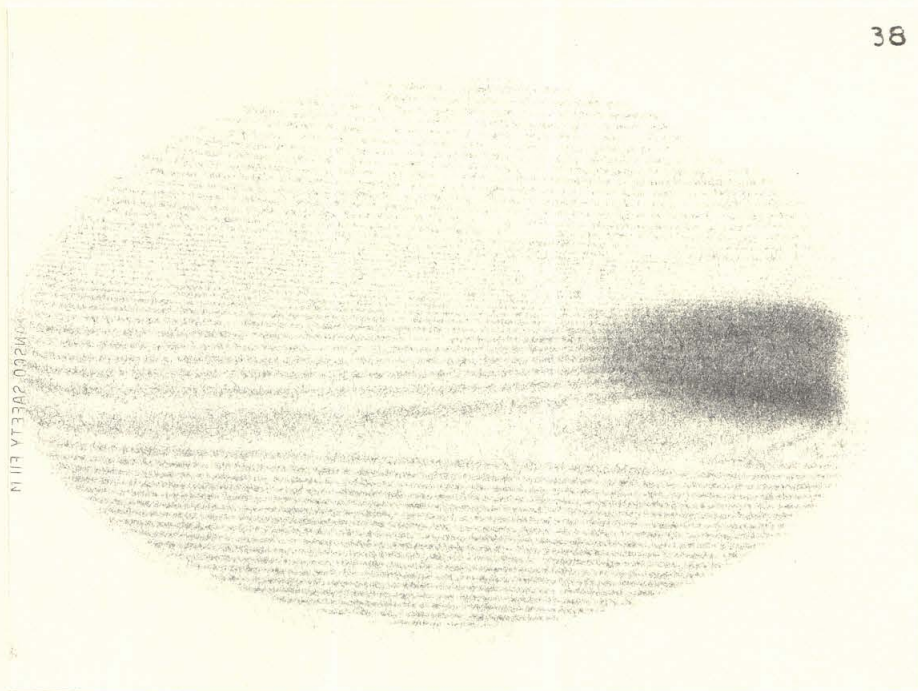


Fig. 4 - Close-up of Plane-Parallel Mirror Frame Showing
Gimbals and Rotating Motors.

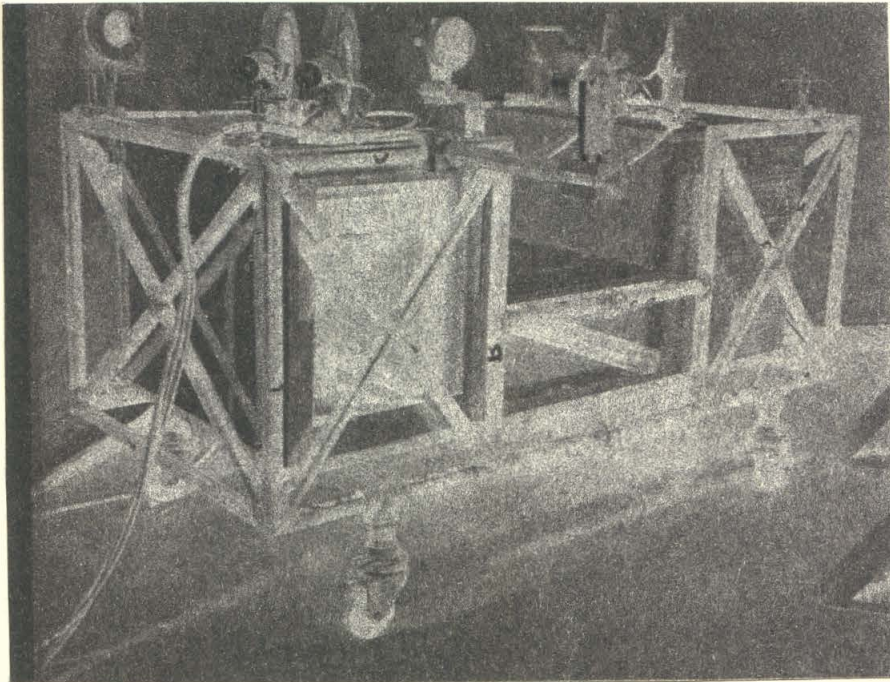


Fig. 5 - Undisturbed Horizontal Fringes

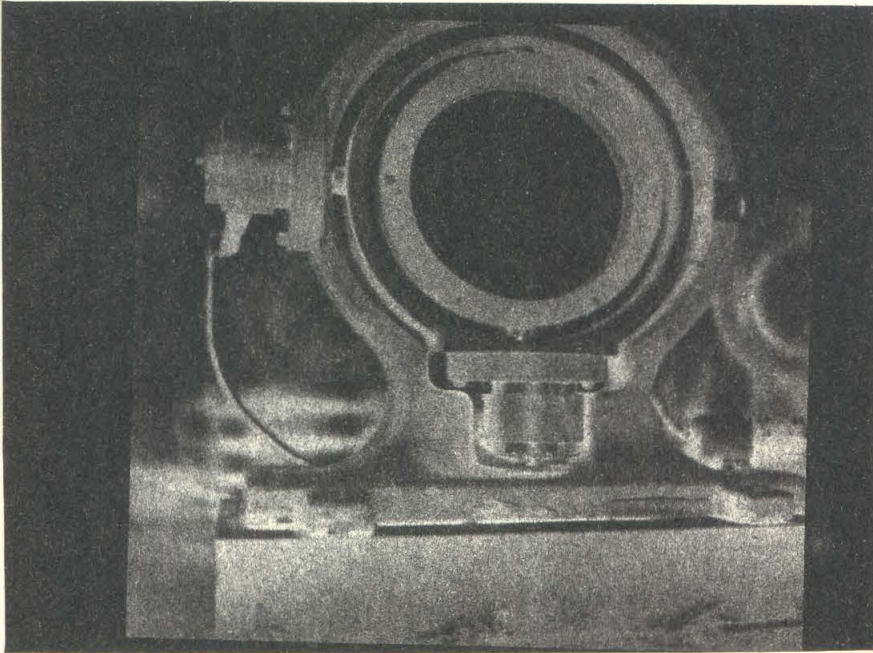


Fig. 6 - Horizontal Fringe Picture of a 10° Semi-Angle
Wedge at $M = 1.28$.

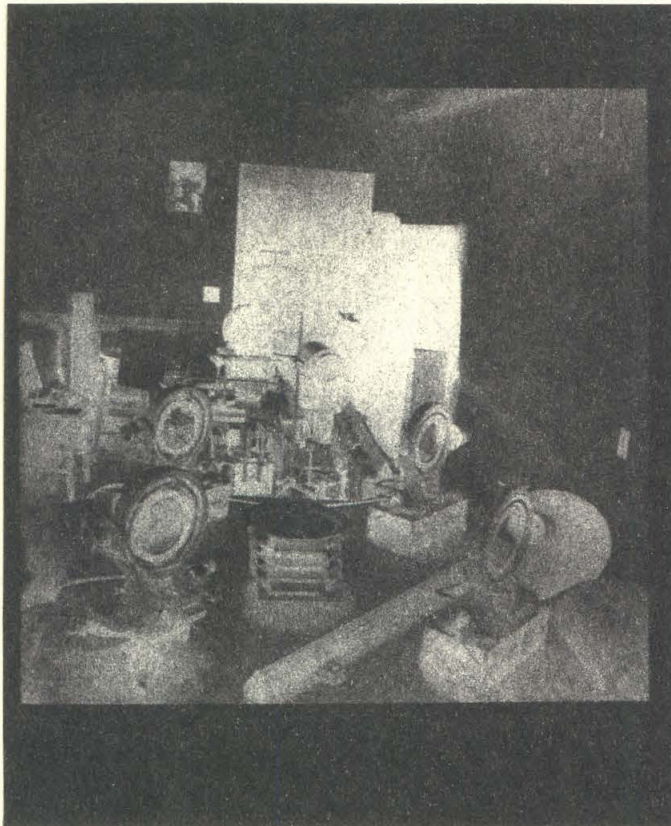


Fig. 7 - Lines of Constant Air Density Made by Superimposing
a Positive of Fig. 5 and a Negative of Fig. 6.



Fig. 8 - Lines of Constant Density by the Method of the Infinite Fringe.

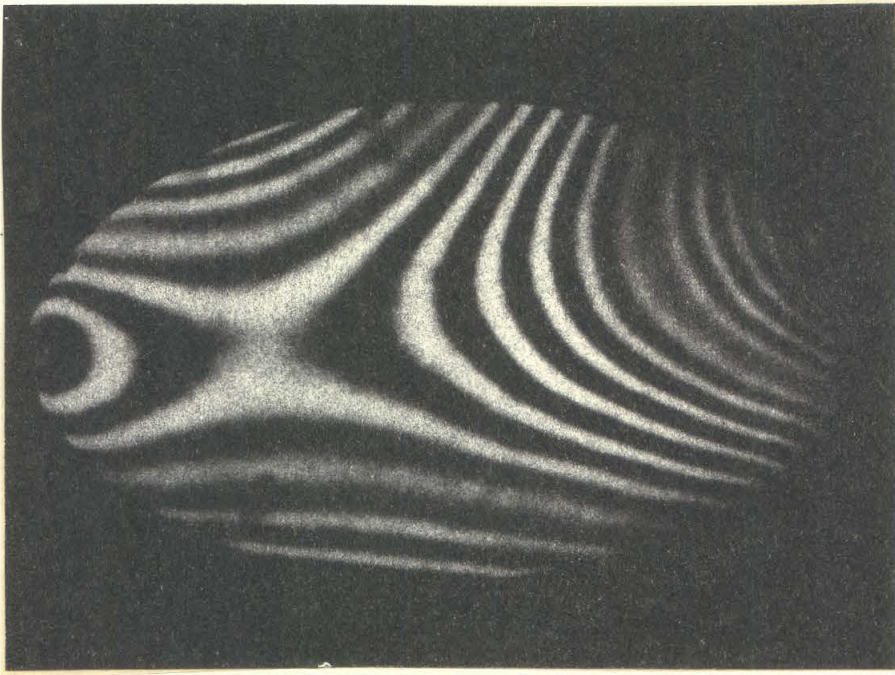


Fig. 9 - White Light Picture Showing How Fringes May be Traced Through a Shock Wave.

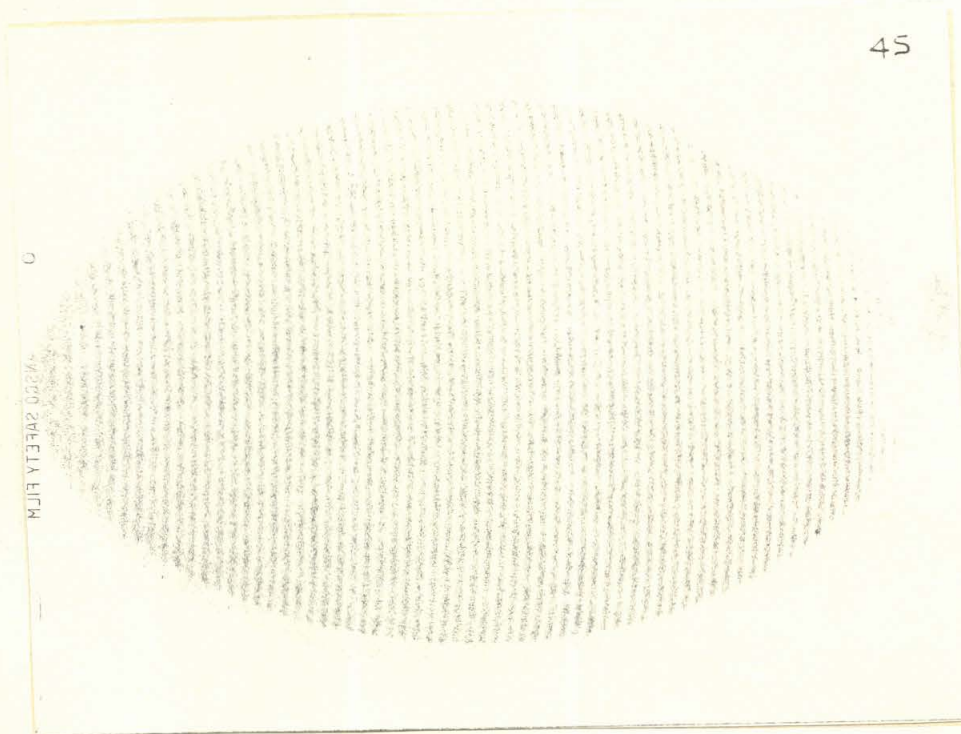


Fig. 10 - Schlieren Picture Made with Knife-Edge Mounted
on the Interferometer.